

Bispectra of Sea-Surface Temperature Anomalies

DETLEV MÜLLER

Climate Dynamics Laboratory, Institute of Geophysics and Planetary Physics, UCLA, Los Angeles, CA 90024

(Manuscript received 1 May 1986, in final form 15 July 1986)

ABSTRACT

Observed anomalies of sea-surface temperatures (SST) exhibit significant triple-correlations and bispectra. Features of this type are not covered by the standard Ornstein Uhlenbeck (OU) concept of SST fluctuations. The present paper derives the spectrum and the bispectrum for a simple non-Gaussian Markov process. It can be shown by means of the inverse modeling technique that this process yields a satisfactory approximation to the spectra and the real part of the bispectra of SST-anomaly data. Moreover, the analysis indicates that the imaginary part of the bispectrum cannot be represented in terms of a single-variable model.

1. Introduction

Due to the pronounced difference in thermal inertia between the upper ocean and the atmosphere, SST anomalies have been successfully modeled in terms of stochastic processes (Frankignoul and Hasselmann, 1977). In the major part of the literature, the deterministic SST dynamics are considered to a first approximation as a stable linear system, while the atmospheric forcing is represented by a Gaussian white noise. In this framework, SST fluctuations become a Gaussian Markov process, or, in the frequency-domain, an ensemble of statistically independent oscillators, which is completely determined if the spectrum is known.

Later, Blaauboer et al. (1982) emphasized that atmospheric variability also affects the linear feedback of the SST dynamics. Moreover, it is well known from mixed-layer theory that large-scale advection as well as turbulent mixing and entrainment processes introduce nonlinear feedbacks into the dynamics of the upper ocean temperature field. In response to Gaussian noises, SST anomalies will hence be non-Gaussian, as it is a matter of longstanding evidence for most geophysical processes (Tukey, 1961). In the frequency domain, this property emerges as an energy transfer among oscillators, which is directly measured by the bispectrum.

$$r_3(t; \omega_1, \omega_2) = \int_{-\infty}^{\infty} d^2\tau e^{i(\omega_1\tau_1 + \omega_2\tau_2)} \langle x(t)x(t+\tau_1)x(t+\tau_2) \rangle \quad (1.1)$$

i.e., the (twofold) Fourier transform of the triple correlation of the SST anomalies $x(t)$.

In the present paper, the bispectrum of a simple non-

Gaussian process will be calculated and compared to observations. As a model the scalar, linear equation will be taken with correlated multiplicative and additive Gaussian white noises. This model is on the borderline of linear and nonlinear systems: while the average dynamics are still linear, the evaluation of its stochastics requires some expansion procedure. The following calculations employ the white-noise limit of the Kubo expansion, which is a time-ordered cumulant expansion with respect to the Kubo number (van Kampen, 1981). General non-Gaussian aspects of the process can then be discussed in the Fokker-Planck (FP) picture (section 2), while the observable correlations and spectra will be derived from the Langevin picture.

For the stationary version of this process the correlation and spectrum have been examined by Blaauboer et al. (1982) stating basically a close resemblance to the corresponding results for the familiar OU-process. In the following the condition of stationarity will be dropped for the forcing noise and a particular non-stationarity, the cyclostationary process will be considered in some detail. The genuine non-Gaussian features of the process appear in the calculation of the triple correlation, which will be performed for the nonstationary case. With specified time dependence of the noise variances, the bispectrum can be obtained from this expression according to (1.1). Here, this will be done for the stationary process (section 3).

Bispectra of observed SST time series can be evaluated on a machine by means of a fast Fourier transform, similar to the well-known computation of ordinary spectra. Data and model are most conveniently compared according to the inverse-modeling technique, thus taking into account the inherent statistical indeterminacy associated with finite datasets (section 4).

2. The model

For an ocean mixed layer of constant depth h , the heat budget per unit horizontal area reads

$$c\rho h\dot{T}_0 = F_q(t, T_0) \quad (2.0)$$

where ρ denotes the density of sea water and c its heat capacity per unit mass. The total heat flux F_q represents exchanges of heat with the atmosphere, with the layer beneath the mixed layer and finally the contributions from large scale advection. Expanding the heat flux with respect to temperature one obtains to first order:

$$\left(\frac{d}{dt} + \lambda_0\right)T_0(t) = F_0(t), \quad (2.1)$$

a linear relaxation equation for the deterministic dynamics of the mixed layer temperature T_0 . In the following, the linear feedback coefficient

$$\lambda_0 = -\partial_{T_0}F_q(T_0 = T_*)/\rho ch = \text{const} > 0$$

evaluated at an appropriate reference temperature T_* , will be considered a positive constant, while the forcing

$$F_0(t) = F_q(t, T_0 = T_*)/\rho ch$$

depends on time.

As a characteristic feature of the heat budget (2.0) there are atmospheric processes and oceanic turbulence involved with correlation times much smaller than the system relaxation time $\tau_0 = 1/\lambda_0$. According to the concept of stochastic climate models (Hasselmann, 1976) this separation in time scales is utilized by embedding the deterministic dynamics (2.1) into a noise ensemble. In particular, the correlation time of the fast processes will be considered approximately zero so that the noises are white. Moreover, they are chosen to be Gaussian in view of the central limit theorem. In the paper at hand the forcing process

$$F(t) = F_0(t) + Y(t)$$

with $\langle Y(t) \rangle = 0$ will be allowed to exhibit nonstationary stochastics

$$\langle Y(t)Y(t+\tau) \rangle = Q_1(t)\delta(\tau)$$

so that the variance $Q_1(t)$ may be an arbitrary non-negative function of time. The feedback process

$$\lambda(t) = \lambda_0 + \gamma_0(t)$$

with $\langle \gamma_0(t) \rangle = 0$ will be assumed stationary:

$$\langle \gamma_0(t)\gamma_0(t+\tau) \rangle = q_0\delta(\tau)$$

with positive and constant variance q_0 . The two processes may be correlated:

$$\langle Y(t)\gamma_0(t+\tau) \rangle = Q_{01}(t)\delta(\tau)$$

where the noise variances are subject to the Cauchy-Schwarz inequality

$$q_0Q_1(t) - Q_{01}^2(t) \geq 0.$$

Thus the stochastic generalization of (2.1) becomes

$$\left[\frac{d}{dt} + \lambda(t)\right]T(t) = F(t). \quad (2.2)$$

Due to the presence of the noise ensemble, the mixed layer temperature has now to be regarded as a stochastic process $T(t) = T_1(t) + x(t)$ with mean $T_1(t) = \langle T(t) \rangle$ and zero average anomaly $x(t) = T(t) - T_1(t)$.

Formally the averaged steady-state solution of (2.2) may be cast into the integral form

$$T_1(t) = \int_{-\infty}^{\infty} dt' \langle \mathcal{G}(t-t')F(t') \rangle \quad (2.2a)$$

where the Green function

$$\mathcal{G}(t-t') = \theta(t-t') \exp\left[-\int_{t'}^t ds \lambda(s)\right] \quad (2.2b)$$

ensures causality by means of the unit-step function $\theta(t-t')$. Since (2.2b) involves the exponential of a stochastic process, the averaging procedure in (2.2a) has to invoke some appropriate expansion technique. It is shown in Appendix A that the Kubo expansion to second order yields for (2.2a)

$$T_1(t) = \int_{-\infty}^{\infty} dt' \mathcal{G}_1(t-t')F_1(t') \quad (2.3a)$$

with

$$\mathcal{G}_1(t-t') = \theta(t-t')e^{-\lambda_1(t-t')} \quad (2.3b)$$

where $\lambda_1 = \lambda_0 - q_0/2$ and

$$F_1(t) = F_0(t) - Q_{01}(t)/2. \quad (2.3c)$$

It follows from (2.3a) that the average mixed layer temperature satisfies the deterministic equation

$$\left(\frac{d}{dt} + \lambda_1\right)T_1(t) = F_1(t) \quad (2.3)$$

which in particular no longer coincides with the noise-free limit (2.1) of the stochastic dynamics (2.2). As the specific feature of multiplicative noise, the averaged forcing and feedback are "renormalized" by the noise variances according to (2.3b) and (2.3c). Physically the "fluctuation-renormalization" increases the system's inertia, since now the average relaxation time $\tau_1 = 1/\lambda_1$ is larger than the noise-free relaxation time $\tau_0 = 1/\lambda_0$.

Subtracting now the average dynamics (2.3) from the stochastic equation (2.2) yields the dynamics of the SST anomalies

$$\left[\frac{d}{dt} + \lambda(t)\right]x(t) = f(t) \quad (2.4)$$

where the effective forcing

$$f(t) = f_0(t) + \gamma(t)$$

has an average

$$f_0(t) = [Q_{01}(t) - q_0T_1(t)]/2$$

superposed by a zero-average Gaussian white noise

$$y(t) = Y(t) - y_0(t)T_1(t). \quad (2.4a)$$

The autocorrelation of this noise is

$$\langle y(t)y(t+\tau) \rangle = q_1(t)\delta(\tau)$$

where its variance $q_1(t)$ is easily determined from the original noises as

$$q_1(t) = q_0T_1^2(t) - 2Q_{01}(t)T_1(t) + Q_1(t),$$

and for its cross-correlation with the feedback noise

$$\langle y(t)y_0(t+\tau) \rangle = q_{01}(t)\delta(\tau)$$

one obtains the covariance

$$q_{01}(t) = Q_{01}(t) - q_0T_1(t) = 2f_0(t).$$

The effective noises satisfy the Cauchy-Schwarz inequality, since

$$q_0q_1(t) - q_{01}^2(t) = q_0Q_1(t) - Q_{01}^2(t) \geq 0.$$

In contrast to linear models with purely additive noise, average dynamics and fluctuations no longer superpose; while the noise stochastics renormalize the average dynamics, the average temperature enters the effective noise (2.4a). This indicates a nonlinear feature of the model at hand.

Some general stochastic properties of the anomaly model (2.4) can be immediately derived from the corresponding FP-equation

$$\partial_t p = \lambda_1 \partial_x (xp) + \frac{1}{2} \partial_x^2 (Qp) \quad (2.5)$$

where

$$Q(t, x) = q_0x^2 - 2q_{01}(t)x + q_1(t)$$

and $p = p(t_0, x_0|t, x)$ denotes the conditional probability density for the anomaly to have the value x at time t given the value x_0 at time $t_0 < t$. This equation may be obtained from the Langevin-picture (2.4) either by expanding the system's Liouville equation with respect to the Kubo-number or, in a more phenomenological way, by means of the Stratonovich-calculus of stochastic differential equations (van Kampen, 1981).

A first simple result from (2.5) is the steady-state solution for the stationary process $q_1 = \text{const}$ and $q_{01} = \text{const}$.

$$p(x) = AQ^{-\mu}(x) \exp[-b_0 \arctan(b_1x - b_2)] \quad (2.5a)$$

with an appropriately chosen normalization constant A and

$$\begin{aligned} \mu &= (\lambda_1 + q_0)/q_0, & b_0 &= 2\lambda_1 b_2/q_0, \\ b_1 &= q_0 b_2/q_{01}, & b_2 &= q_{01}(q_0 q_1 - q_{01}^2)^{-1/2}. \end{aligned}$$

For vanishing feedback noise: $q_0 \rightarrow 0$ and $q_1 \rightarrow Q_1$ this density reduces to the familiar Gaussian

$$p(x) = (\lambda_0/\pi Q_1)^{1/2} \exp(-\lambda_0 x^2/Q_1).$$

Inspection of Fig. 1 clearly shows that the distinctive difference between the stationary anomaly (2.5a) and a Gaussian model is loss of symmetry with respect to the mean mixed layer temperature T_1 : $p(x) \neq p(-x)$. Its most probable value

$$\max p(x) = p(x = q_{01}/q_0\mu)$$

is essentially determined by the cross-correlation of the feedback noise and the effective forcing noise. If this cross-correlation vanishes, which does not imply vanishing feedback noise, fluctuations become symmetric with respect to the mean temperature

$$p(x) = (q_0/\pi)^{1/2} \Gamma(\mu) \Gamma^{-1}(\nu) q_1^\nu Q^{-\mu}(x), \quad (2.5b)$$

since now

$$Q(x) = q_1 + q_0x^2 = Q(-x).$$

As for the above densities, the normalization of (2.5b) has been chosen for $x \in (-\infty, \infty)$, Γ denotes the Eulerian Gamma function and $\nu = \mu^{-1/2} = \lambda_0/q_0$. The non-Gaussian feature of (2.5b) is its slower asymptotic decay, i.e., Gaussian SST anomalies exhibit a higher concentration toward the mean temperature.

Furthermore, the FP-equation immediately yields the moment dynamics for $r_n(t) := \langle x^n(t) \rangle$. Integrating by parts, one obtains from (2.5)

$$\left(\frac{d}{dt} + \lambda_n \right) r_{n0}(t) = f_{n0}(t) \quad (2.6)$$

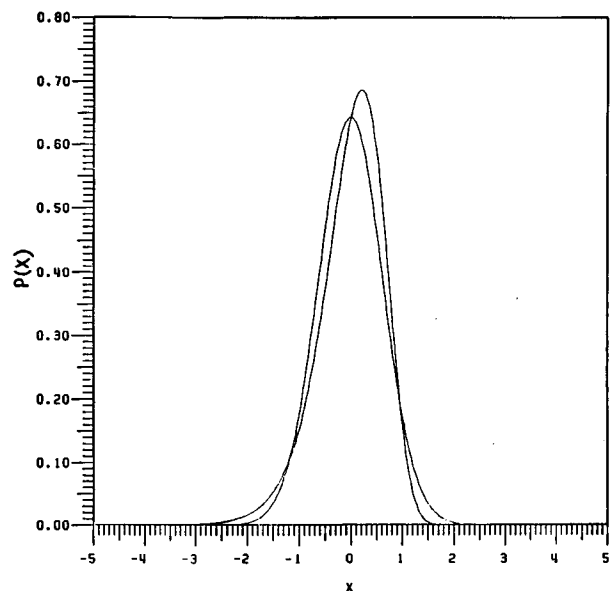


FIG. 1. Probability densities in the stationary case. The symmetric curve is the Gaussian, the asymmetric curve is the density (2.5a).

where

$$\lambda_n = n \left(\lambda_0 - \frac{n}{2} q_0 \right)$$

$$f_{k0}(t) = k(k-1) \left[\frac{1}{2} q_1(t) r_{j0}(t) - q_{01}(t) r_{j0}(t) \right],$$

$$i = k-2, \quad j = k-1.$$

The integral version of (2.6) reads

$$r_{n0}(t) = \int_{-\infty}^{\infty} dt' \mathcal{G}_{n0}(t-t') f_{n0}(t')$$

with Green functions

$$\mathcal{G}_{n0}(t-t') = \theta(t-t') e^{-\lambda_n(t-t')}.$$

These Green functions increase exponentially in time for $n > 2\lambda_0/q_0$ so that the dynamics of the higher moments becomes unstable. In fact, the multiplicative noise will eventually drive the system into its unstable regime, and these events dominate the time-development of the higher moments. An extreme example of this type of stochastics is known from the Wiener process, which has been discussed in a geophysical context by Hasselmann (1976). This process exhibits a stable first moment, while its variance increases linearly in time. In these cases the steady-state problem is not well defined. An extensive study of the problem of stochastic stability can be found in Arnold (1974).

In contrast to Gaussian SST anomalies, the present model exhibits nonvanishing odd moments, as long as $q_{01}(t) \neq 0$. These are essentially associated with the asymmetry of the anomalies with respect to T_1 . But similar to the Gaussian case, the knowledge of the first few moments, namely the first three, determines the moment algebra completely. For later reference, the variance

$$r_{20}(t) = \int_{-\infty}^{\infty} dt' \mathcal{G}_{20}(t-t') q_0(t') \quad (2.7)$$

and the third moment

$$r_{30}(t) = -6 \int_{-\infty}^{\infty} dt' \mathcal{G}_{30}(t-t') q_{01}(t') r_{20}(t') \quad (2.8)$$

are explicitly written.

3. Correlations and spectra

Since correlation functions and spectra can be directly obtained from observed SST time series, they provide the crucial link between data and model. In particular they yield a far more sensitive representation of the anomaly stochastics than histogram techniques. In the following, these quantities shall be discussed for the model under consideration.

By definition, one has for the correlation

$$r_2(t_1, t_2) = \langle x(t_1)x(t_2) \rangle = \int_{-\infty}^{\infty} d^2t' \langle h(t'_1, t_1)h(t'_2, t_2) \rangle \quad (3.1a)$$

where

$$h(t', t) = \mathcal{G}(t-t')f(t') \quad (3.1b)$$

and the short-hand notation d^2t , has been used, although the two integrations do not commute, but depend on the relative order of t_1 and t_2 . For the stationary process, (3.1a) has been calculated to second-order Kubo-number by Blaauboer et al. (1982). Using (2.7) and $\tau = t_2 - t_1$ a straightforward generalization yields for the present nonstationary process

$$r_2(t, \tau) = r_{20} \left(t + \frac{1}{2}\tau - \frac{1}{2}|\tau| \right) \mathcal{G}_1^+(\tau) \quad (3.1)$$

where

$$\mathcal{G}_1^+(\tau) = \mathcal{G}_1(\tau) + \mathcal{G}_1(-\tau) = e^{-\lambda_1|\tau|} = \mathcal{G}_1^+(-\tau)$$

denotes the symmetrized Green function of the average dynamics of the mixed layer temperature (2.3) while the argument of the variance selects the earlier of the two times t and $t + \tau$

$$\min(t, t + \tau) = t + \frac{1}{2}\tau - \frac{1}{2}|\tau|.$$

The particular form of (3.1) is frequently referred to as “fluctuation–dissipation relation” (Leith, 1975): the correlation of anomalies is determined by their stochastics at one instant (“fluctuation”), while its temporal behavior with respect to the time-lag solely depends on the dynamics of the mean temperature (“dissipation”). The factorization of the correlation (3.1) is basically due to the time-independent feedback stochastics in the present model. For nonstationary feedback, the correlation function becomes a convolution-type product. A Gaussian process of this kind with application to SST anomalies has been discussed by Elvira and Lemke (1982).

In the stationary case, (3.1) reduces to

$$r_2(\tau) = r_{20} \mathcal{G}_1^+(\tau) = (q_1/\lambda_2) e^{-\lambda_1|\tau|}$$

displaying the symmetry

$$r_2(\tau) = r_2(-\tau)$$

as necessary for a stationary process. For the spectrum, one obtains

$$r_2(\omega) = \int_{-\infty}^{\infty} d\tau e^{i\omega\tau} r_2(\tau) = 2\lambda_1 r_{20} (\lambda_1^2 + \omega^2)^{-1} = r_2(-\omega). \quad (3.1c)$$

These are the results derived by Blaauboer et al. (1982). The spectrum of the stationary non-Gaussian Markov process is continuous and red, i.e., spectral energy con-

centrates at low frequencies. As for the OU-process, the present system develops long-term variability in response to white noises. In distinction to the OU-case, the meaning of the spectrum parameters has been slightly changed by "fluctuation renormalization." As far as the spectrum is concerned the difference between the two processes is thus of minor significance.

A nonstationary situation with relevance to SST anomalies is that of seasonally varying forcing variance. It is well known that the heat exchange of the mixed layer with the atmosphere and the thermocline is subject to much larger fluctuations in spring than in late summer, for instance. This can be taken account of by considering the forcing variance as a periodic function that hence has a representation in terms of a Fourier series

$$q_1(t) = \sum_{\nu} e^{-i\nu\omega_0 t} q_1^{\nu} \quad (3.2a)$$

where $\omega_0 = 2\pi/T_0$ for some characteristic period T_0 , 1 year say, and the Fourier coefficients are conversely given as

$$q_1^{\nu} = \frac{1}{T_0} \int_0^{T_0} dt e^{i\nu\omega_0 t} q_1(t).$$

Stochastic processes of this type are called "cyclostationary" and have originally been discussed in econometrics (Parzen and Pagano, 1979). Their importance in geophysics has been demonstrated by Hasselmann and Barnett (1981).

Inserting (3.2a) into (2.7) one obtains for the variance of the cyclostationary non-Gaussian Markov process

$$r_{20}(t) = \sum_{\nu} e^{-i\nu\omega_0 t} r_{20}^{\nu} \quad (3.2b)$$

with coefficients

$$r_{20}^{\nu} = q_1^{\nu} (\lambda_2 - i\nu\omega_0)^{-1}.$$

With the variance (3.2b) the correlation (3.1) becomes

$$r_2(t, \tau) = \sum_{\nu} e^{-i\nu\omega_0 t} r_2^{\nu}(\tau) \quad (3.2)$$

where

$$r_2^{\nu}(\tau) = r_{20}^{\nu} \exp\left[-\frac{1}{2} i\nu\omega_0(\tau - |\tau|)\right] \mathcal{G}_1^+(\tau)$$

exhibiting the symmetry

$$\text{c.c. } r_2^{\nu}(\tau) = r_2^{-\nu}(\tau).$$

As the characteristic nonstationary feature, this correlation no longer depends on the time lag only. Rather, it is represented by a Fourier-series with respect to the seasonal time, while the lag dependence is completely shifted to the expansion coefficients. For $\nu = 0$ the stationary case is recovered. The first few coefficients are shown in Fig. 2.

The spectrum of the process

$$r_2(t, \omega) = \sum_{\nu} e^{-i\nu\omega_0 t} r_2^{\nu}(\omega) \quad (3.3)$$

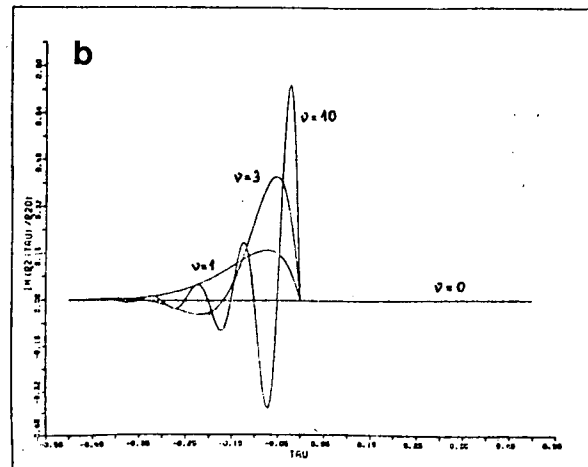
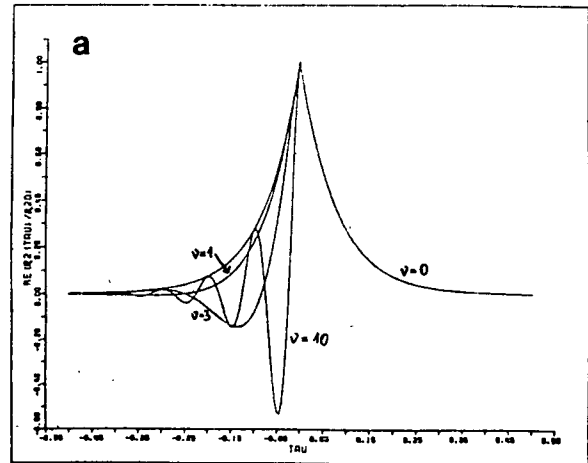


FIG. 2. The cyclostationary process: (a) $\text{Re}(r_2^{\nu}(\tau)/r_{20}^{\nu})$ and (b) $\text{Im}(r_2^{\nu}(\tau)/r_{20}^{\nu})$ for $\nu = 0, 1, 3, 10$.

with

$$r_2^{\nu}(\omega) = r_{20}^{\nu} (2\lambda_1 - i\nu\omega_0) \{(\lambda_1 - i\omega)[\lambda_1 + i(\omega - \nu\omega_0)]\}^{-1}$$

is seen to vary in the course of the seasons. Again, for $\nu = 0$ the stationary spectrum (3.1c) is recovered from (3.3). Instead of reading (3.3) as a time-dependent spectrum, an additional Fourier transformation with respect to the seasonal time

$$r_2(\Omega, \omega) = \sum_{\nu} \delta(\Omega - \nu\omega_0) r_2^{\nu}(\omega)$$

suggests a different interpretation. While $r_2^{\nu}(\omega)$ is a continuous function of frequency, the δ function introduces discrete lines into the spectrum. It may thus be visualized as a band-spectrum with bands $r_2^{\nu}(\omega)$ centered at $\Omega = \nu\omega_0$.

The non-Gaussian nature of the present process manifests itself essentially in the nonvanishing triple correlation and bispectrum. These are associated with

the skewness of the SST anomalies with respect to the mean temperature T_1 , as indicated for the stationary case by (2.5a). Only in very extreme cases one may expect to detect such an asymmetry from SST data by visual inspection or histogram techniques and thus the bispectrum is the most convenient measure for deviations from Gaussian behavior.

For the triple correlation one has by definition

$$r_3(t_1, t_2, t_3) = \langle x(t_1)x(t_2)x(t_3) \rangle \\ = \int_{-\infty}^{\infty} d^3t' \langle h(t'_1, t_1)h(t'_2, t_2)h(t'_3, t_3) \rangle \quad (3.4a)$$

where $h(t', t)$ is given by (3.1b) and the abbreviation d^3t' has been used although the three integrations do not commute. It is shown in appendix B that the triple correlation of the present nonstationary, non-Gaussian Markov process becomes to second-order Kubo number

$$r_3(t_1 \leq t_2 \leq t_3) = \mathcal{G}_1(t_3 - t_2) \left[\mathcal{G}_{20}(t_2 - t_1)r_{30}(t_1) \right. \\ \left. - 2r_{20}(t_1) \int_{t_1}^{t_2} dt' \mathcal{G}_{20}(t_2 - t') \mathcal{G}_1(t' - t_1)q_{01}(t') \right]. \quad (3.4)$$

The corresponding expressions for time orders other than the one indicated can be immediately obtained from (3.4). As for the correlation function (3.1), the moments $r_{20}(t)$ and $r_{30}(t)$ of the anomalies enter the triple correlation only at the earliest time t_1 , while its temporal behavior with respect to the time-lags now depends on the Green functions \mathcal{G}_1 of the mean temperature and the Green function \mathcal{G}_{20} of the anomaly variance.

In the stationary case the triple correlation can be largely simplified. Then, from (2.8)

$$r_{30} = -6q_{01}r_{20}/\lambda_3$$

and the convolution integral in (3.4) can be performed, yielding

$$r_3(t_1 \leq t_2 \leq t_3) = r_{30}\mathcal{G}_1(t_3 - t_1)$$

which is in particular independent of the intermediate time t_2 . Introducing the time-lags $\tau_1 = t_2 - t_1$ and $\tau_2 = t_3 - t_1$ as well as

$$\mu(\tau_1, \tau_2) = \max(t_\nu) - \min(t_\nu) = \frac{1}{2}(|\tau_1| + |\tau_2| + |\tau_1 - \tau_2|),$$

this may be written independent of chronology

$$r_3(\tau_1, \tau_2) = r_{30}e^{-\lambda_1\mu} \\ = r_{30}\mathcal{G}_1\left(\frac{1}{2}\tau_1\right)\mathcal{G}_1\left(\frac{1}{2}\tau_2\right)\mathcal{G}_1\left[\frac{1}{2}(\tau_1 - \tau_2)\right]. \quad (3.5)$$

As is well known (Hasselmann et al., 1963), the triple correlation of a stationary process displays the symmetries

$$r_3(\tau_1, \tau_2) = r_3(\tau_2, \tau_1) = r_3(\tau_1 - \tau_2, -\tau_2),$$

which are readily verified for (3.5). In addition, it is found that (3.5) satisfies

$$r_3(\tau_1, \tau_2) = r_3(-\tau_1, -\tau_2). \quad (3.5a)$$

This ‘‘reversibility’’ is due to the lack of any memory effects in the present model.

In the frequency domain the SST anomalies are visualized as an ensemble of oscillations and the bispectrum measures the transfer of energy among these oscillators. For independent oscillators (e.g., the Gaussian case) the bispectrum trivially vanishes. In the present case one obtains upon insertion of (3.5) into (1.1)

$$r_3(\omega_1, \omega_2) = 2\lambda_1^2 r_{30}(3\lambda_1^2 + \omega_1^2 + \omega_2^2 + \omega_1\omega_2)/\mathcal{D}(\omega_1, \omega_2) \quad (3.6)$$

with denominator

$$\mathcal{D}(\omega_1, \omega_2) = (\lambda_1^2 + \omega_1^2)(\lambda_1^2 + \omega_2^2)(\lambda_1^2 + (\omega_1 + \omega_2)^2).$$

In the frequency domain the stationarity of the process is reflected by the symmetries (Hasselmann et al., 1963)

$$r_3(\omega_1, \omega_2) = r_3(\omega_2, \omega_1) = r_3[\omega_1, -(\omega_1 + \omega_2)].$$

As a consequence of (3.5a)

$$\text{Im}r_3(\omega_1, \omega_2) = 0;$$

i.e., for the present process the bispectrum is solely real. Thus, the imaginary part of the bispectrum provides a measure for the presence of memory effects. Figure 3 shows an isoline representation of (3.6).

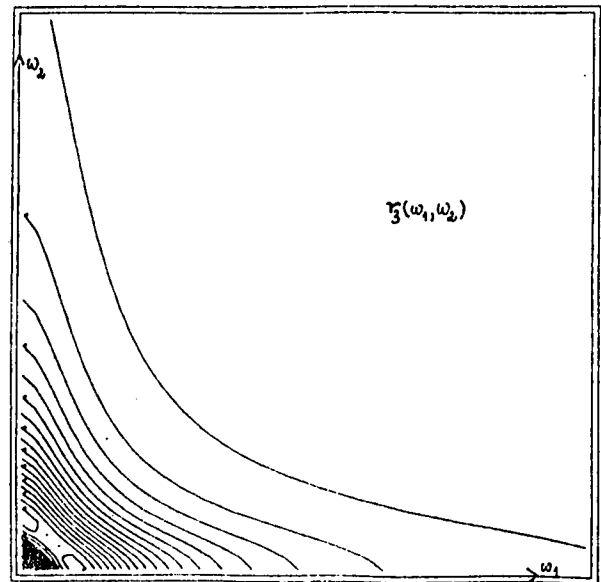


FIG. 3. Model bispectrum of the stationary non-Gaussian process with $r_{30} = 0.1 \text{ K}^3$ and $\lambda_1 = 10 \text{ y}^{-1}$. The frequency scale of abscissa and ordinate is given by (4.4).

4. Inverse modeling of spectra and bispectra

The practical relevance of the above model is conveniently tested against data in the frequency domain. The data provided by the British Meteorological Office were time series of upper ocean temperature profiles $T(t, -275 \text{ m} \leq z \leq 0 \text{ m})$, recorded at North Atlantic weathership stations D, located at $44^\circ\text{N}, 41^\circ\text{W}$, I ($59^\circ\text{N}, 19^\circ\text{W}$) and K ($45^\circ\text{N}, 16^\circ\text{W}$). Each of the profiles represented an average over $\mathcal{DT} = 5$ days and the total time series cover a period of about eight years.

SST in the narrow sense, i.e., profile values $T(t, z = 0 \text{ m})$, will generally be affected by local influences as well as by large scale horizontal advection. In view of the physical limitations of the model considered, it can hardly be expected to give a proper representation of advective effects. According to Gill and Turner (1976) a certain elimination of these can be achieved with

$$X(t) = T(t, z = 0 \text{ m}) - T(t, z = -275 \text{ m}) \quad (4.1)$$

thus subtracting variations that extend homogeneously over the whole column. From the series $X(t)$ the average seasonal cycle $T_1(t) = \langle X(t) \rangle$ can now be determined such that the anomaly

$$x(t) = X(t) - T_1(t)$$

has zero average. The data spectrum is then obtained from the blockwise Fourier transform $x_k(\omega)$ of the SST anomaly $x(t)$ according to

$$X_2(\omega)\omega_{\min} = (\text{KCH})^{-1} \sum_{k=1}^{\text{KCH}} x_k(\omega)x_k^*(\omega) \quad (4.2)$$

while the bispectrum becomes

$$X_3(\omega_1, \omega_2)\omega_{\min}^2 = (\text{KCH})^{-1} \sum_{k=1}^{\text{KCH}} x_k(\omega_1)x_k(\omega_2)x_k^*(\omega_1 + \omega_2). \quad (4.3)$$

Here, KCH denotes the number of blocks of length LCH and

$$\omega_{\min} = 2\pi/\text{LCH} \leq \omega \leq \omega_{\max} = \pi/\mathcal{DT}. \quad (4.4)$$

A careful discussion of the normalization conditions these data spectra and bispectra satisfy can be found in Hasselmann et al. (1963). The real and imaginary part of the bispectra, thus obtained for weatherships D, I and K, are shown in Figs. 4. Note that all three cases clearly exhibit a nontrivial imaginary part.

The comparison of data spectra and bispectra with the present model in the framework of the inverse modeling technique employs an "optimal-model" algorithm and the concepts of statistical inference. The optimal-model algorithm is taken to be the standard least-square fit in the following and provides numerical values P_μ for the parameter vector p_μ . The statistical concepts yield confidence intervals for the parameters

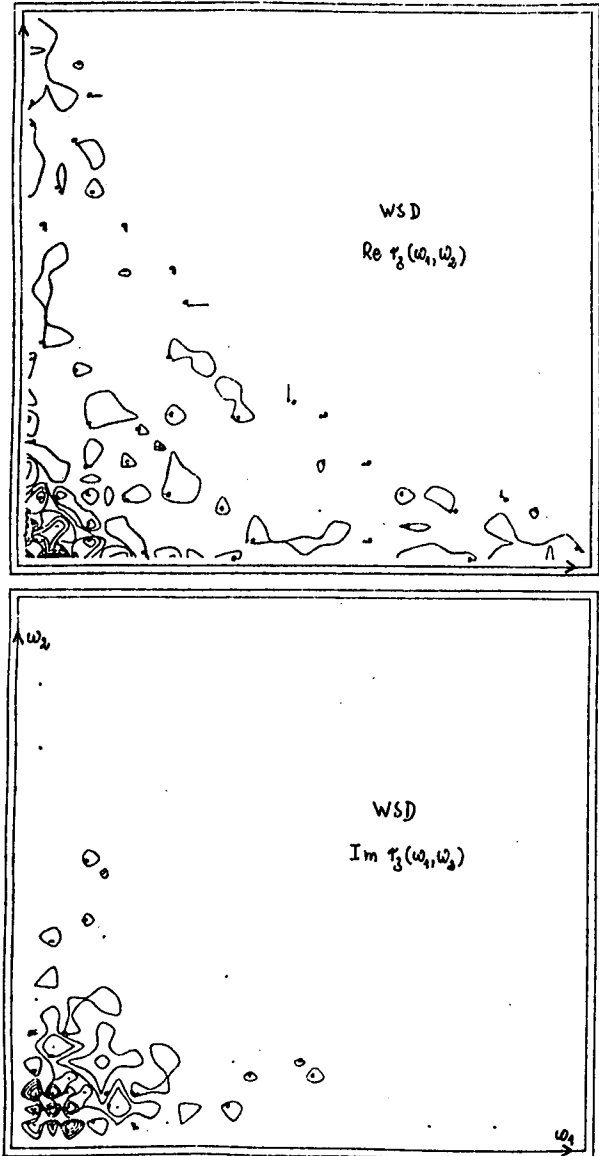


FIG. 4a. Real and imaginary part of data bispectrum at weathership D. Scales as in Fig. 3.

$p_\mu = P_\mu \pm \Delta P_\mu$ as well as an estimate of the model significance. To this end the data are considered as only one realization out of an ensemble of datasets. In principle the statistics of this ensemble are not available and have to be estimated from the known data. As a consequence of the introduction of the data ensemble, all quantities of the optimal model algorithm become statistics.

In case of the spectrum (3.1c) the parameter vector is

$$p_\mu = (2\lambda_1 r_{20}, \lambda_1)$$

and the optimal model is defined by

$$\epsilon^2(p_\mu = P_\mu) = W^{mn} \epsilon_m \epsilon_n = \min$$

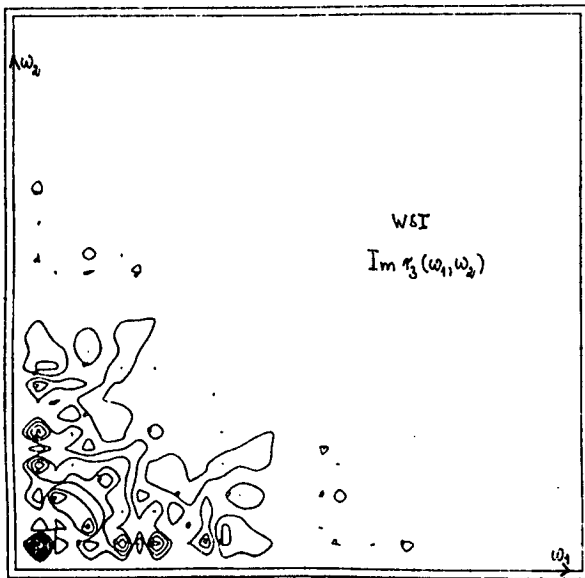
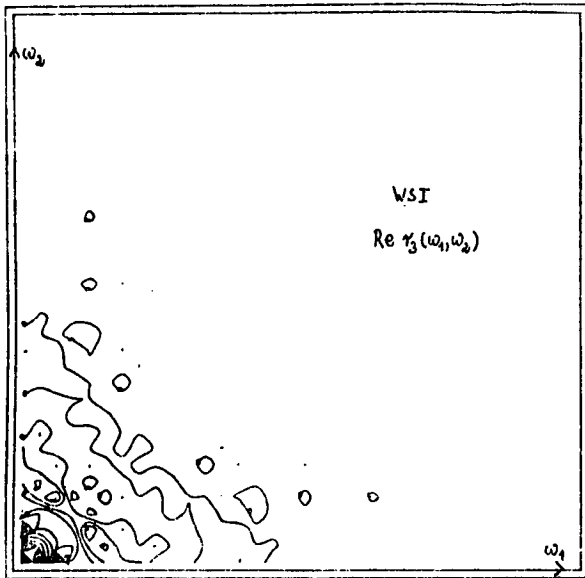


FIG. 4b. As in Fig. 4a but at weather ship I.

where the summation convention is implied and

$$\epsilon_n = X_2(\omega_n) - r_2(\omega_n; P_\mu)$$

is the error function, while the weight matrix is chosen as the inverse of the data-covariance matrix

$$W_{mn} = \langle\langle X_2(\omega_m) X_2(\omega_n) \rangle\rangle^{-1}.$$

An estimate for this matrix can be obtained from (4.2), using the occurrence of only positive frequencies and the statistical independence of blocks

$$\langle\langle X_2(\omega_m) X_2(\omega_n) \rangle\rangle = r_2^2(\omega_m) \delta_{mn} / KCH.$$

Furthermore, it is assumed that ϵ^2 is χ^2 -distributed with

$$\langle \epsilon^2 \rangle = N - M$$

degrees of freedom, where N denotes the dimension of the data vector and M that of the parameter vector. With an a priori specified significance level, 95% say, a critical ϵ_c^2 can now be determined for the known χ^2 -distribution, such that $\epsilon^2 > \epsilon_c^2$ occurs at a frequency of 5%, while all $\epsilon^2 < \epsilon_c^2$ occur at a frequency of 95%. The data are then said to falsify the model, if $\epsilon^2 (p = P) > \epsilon_c^2$, while the model has not to be rejected, if $\epsilon^2 (p = P) < \epsilon_c^2$. Thus the significance level provides a statistical measure of the degree of detail, the model is required to reproduce with respect to the data.

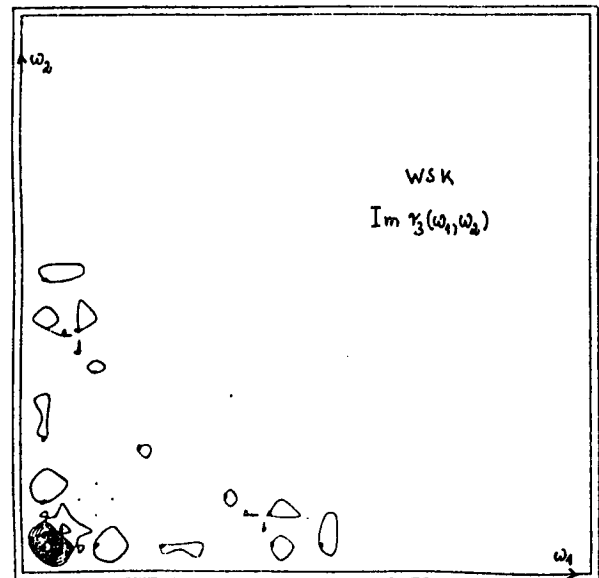
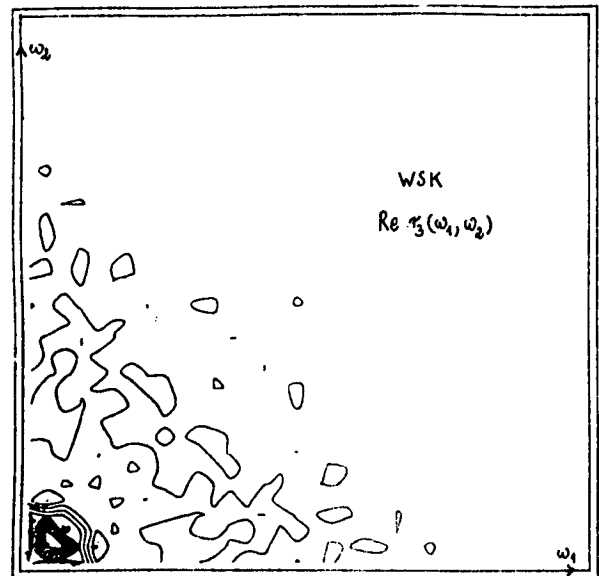


FIG. 4c. As in Fig. 4a but at weather ship K.

For the SST anomaly spectrum at weathership D this procedure yields

$$p_\mu = [(37.9 \pm 4.8)k^2y^{-1}, (11.1 \pm 2.0)y^{-1}], \quad \epsilon^2/\epsilon_c^2 = 0.48$$

and at weathership I

$$p_\mu = [(6.7 \pm 0.9)k^2y^{-1}, (16.5 \pm 2.5)y^{-1}], \quad \epsilon^2/\epsilon_c^2 = 0.38$$

and finally at weathership K

$$p_\mu = [(10.3 \pm 1.2)k^2y^{-1}, (12.2 \pm 1.9)y^{-1}], \quad \epsilon^2/\epsilon_c^2 = 0.82.$$

It is seen from these figures that for none of the weatherships the model has to be rejected at the 95% significance level. This reflects essentially the fact that the non-Gaussian features of the present model do not affect the continuous and red nature of the spectrum, which is widely observed for SST anomalies. On the other hand, the above feedbacks, varying around $\lambda_1 = 13.3y^{-1}$ are about five times larger than the value $\lambda = 2.7y^{-1}$, observed by Frankignoul and Hasselmann (1977) at weathership I. This discrepancy is not associated with their Gaussian and the present non-Gaussian model. In fact, on the mere basis of spectra there is no way to discriminate statistically meaningful between the two models. Rather, their calculations refer to SST in the narrow sense, while the above figures have been obtained from SST, defined by (4.1). This smoothing of the data by elimination of a certain amount of variability leads to a decrease of the observed relaxation time $\tau = 1/\lambda_1$. As a check, the spectrum of weathership I has been recalculated, also using SST in the narrow sense. Now the inverse modeling procedure yields a value $\lambda_1 = 3.1y^{-1}$ in satisfactory agreement with $\lambda = 2.7y^{-1}$. For bispectra the above formalism needs a slight generalization. The optimal model is now determined from

$$\epsilon^2(p_\mu = P_\mu) = W^{klmn} \epsilon_{kl} \epsilon_{mn} = \min$$

with an error matrix

$$\epsilon_{mn} = X_3(\omega_m, \omega_n) - r_3(\omega_m, \omega_n; p_\mu)$$

and a weight tensor

$$W_{klmn} = \langle \langle X_3(\omega_m, \omega_n) X_3(\omega_k, \omega_l) \rangle \rangle^{-1}.$$

Along the same arguments as in the spectrum case and additionally employing the symmetries of (4.3) it is found that

$$\langle \langle X_3(\omega_k, \omega_l) X_3(\omega_m, \omega_n) \rangle \rangle = 5r_3^2(\omega_m, \omega_n) \delta_{km} \delta_{ln} / KCH.$$

For the parameter vector $p_\mu = (r_{30}, \lambda_1)$ inverse modeling of the real part of the bispectra then yields for weathership D

$$p_\mu = [(0.06 \pm 0.01)k^3, (7.7 \pm 2.0)y^{-1}], \quad \epsilon^2/\epsilon_c^2 = 0.87$$

and for weathership I

$$p_\mu = [(0.05 \pm 0.01)k^3, (11.6 \pm 3.2)y^{-1}], \quad \epsilon^2/\epsilon_c^2 = 0.91$$

and finally for weathership K

$$p_\mu = [(0.12 \pm 0.02)k^3, (10.3 \pm 2.9)y^{-1}], \quad \epsilon^2/\epsilon_c^2 = 0.83.$$

These figures indicate that the model is significant at the 95% level, although it may be mentioned that this was not the case for similar computations for a time series from weathership C. In view of higher-order spectra, the present data base should thus be considered only sufficient for qualitative conclusions and the given numbers just represent rough estimates.

For the above cases the third moment r_{30} is always positive, which implies a negative cross-correlation q_{01} between the feedback and the effective forcing. Hence the most probable value of the anomalies is smaller than their average. In the time-domain, this may be visualized as a dominantly Gaussian fluctuation, which in addition exhibits occasionally larger amplitude excursions preferably into the positive direction. This is reminiscent of the phenomenon of intermittency, frequently observed in time series from turbulent systems.

The above values of the feedback parameter λ_1 exhibit reasonable coincidence with the corresponding values, determined from the spectra. Finally, the imaginary part of the bispectra, observed for all weatherships, clearly shows that memory effects do play a role in the dynamics of SST anomalies. These are not covered by the present model.

5. Conclusions

Beside the familiar spectra, weathership data of SST anomalies yield bispectra, exhibiting a significant real and imaginary part. This clearly demonstrates the presence of non-Gaussian effects in the stochastics of these anomalies. A closer empirical examination of non-Gaussian fluctuations requires essentially the evaluation of higher-order spectra from SST data and thus much larger time series of observations.

As a simple theoretical approach the linear relaxation equation with multiplicative and additive noise is considered. The resulting process has the advantage that its non-Gaussian properties do not affect the well-established continuous and red behavior of the spectrum. Moreover, its characteristic skewness is relevant for observed SST-anomalies, as indicated by the real part of data bispectra. On the other hand, the model fails to reproduce a nontrivial imaginary bispectrum due to the lack of memory effects. A generalization that merely introduces memory effects (e.g., a red noise) into the present model would hardly improve the situation. In this case the model anomaly would cease to be Markovian, and processes of this type are theoretically poorly understood. However, memory effects can be modeled in the framework of Markovian processes in terms of coupled, multivariable systems, embedded in a white noise ensemble. Deterministic "skeletons" of this type of model are provided by oceanography in

the form of mixed layer models, including the dynamics of the mixed layer depth and the advecting velocity fields. More realistic models of non-Gaussian features of SST anomalies can thus be expected from the investigation of the stochastic properties of existing mixed layer models.

Acknowledgments. The author would like to thank Professor K. Hasselmann and Dr. K. Herterich for many helpful discussions. Most of this work was performed during the author's stay at the Max Planck Institut für Meteorologie, Hamburg, FRG. Thanks are also due to Professor M. Ghil who carefully read the manuscript. It is a particular pleasure to thank D. Deutsch for typing the manuscript quickly and efficiently. This work is supported by U.S. National Science Foundation Grant ATM 85-14731.

APPENDIX A

The Kubo Expansion

The Kubo expansion is extensively discussed by van Kampen (1981) and its application to the derivation of the correlation function can be found in Blaauboer et al. (1982). Since this expansion technique is not a standard concept in geophysics, its basic ingredients are reviewed in the following derivation of the model dynamics of the mean mixed layer temperature.

The expansion of the exponential of a statistic (2.2b) in terms of cumulants avoids the divergence problem of a moment expansion in steady-state problems. Cumulants will be denoted by double brackets and are defined as

$$\ln \langle e^{\epsilon \Lambda} \rangle =: \sum_{n=1}^{\infty} \frac{\epsilon^n}{n!} \langle\langle \Lambda^n \rangle\rangle.$$

It can be shown that they are certain algebraic combinations of the moments, which vanish to all orders higher than the second for a Gaussian variable. Cumulants are thus particularly designed to measure deviations from Gaussian behavior. For (2.2b) with

$$\mathcal{G}_1(t-t') = \langle \mathcal{G}(t-t') \rangle$$

this yields

$$\mathcal{G}_1(t-t') = \theta(t-t') \exp \left[-\langle\langle \Lambda \rangle\rangle + \frac{1}{2} \langle\langle \Lambda^2 \rangle\rangle + \dots \right] \quad (A1)$$

where

$$\left. \begin{aligned} \langle\langle \Lambda \rangle\rangle &= \int_{t'}^t ds \langle \lambda(s) \rangle = \lambda_0(t-t') \\ \langle\langle \Lambda^2 \rangle\rangle &= \int_{t'}^t d^2s \langle y_0(s_1) y_0(s_2) \rangle \end{aligned} \right\} \quad (A2)$$

If the process $y_0(t)$ were not a white noise, but had a finite autocorrelation time τ_c and an amplitude α , the integral (A2) is of order $\alpha^2(t-t')\tau_c$. Thus, the Kubo number $\alpha\tau_c$ emerges as the relevant expansion param-

eter in (A1). In the white-noise limit: $\tau_c \rightarrow 0$, which is formally balanced by $\alpha \rightarrow \infty$ such that $\alpha^2\tau_c$ remains finite. The Kubo number will be suppressed in the following.

To evaluate (A2) introduce the unit indicator

$$u(s_1) = \int_{t'}^t ds_2 \delta(s_1 - s_2) = \begin{cases} 1, & \text{if } s_1 \in (t', t) \\ 0.5, & \text{if } s_1 = t' \text{ or } s_1 = t \\ 0, & \text{otherwise} \end{cases} \quad (A3)$$

indicating whether its argument s_1 lies within the interval (t', t) , on its boundaries or outside. With the help of the indicator, (A2) becomes

$$\langle\langle \Lambda^2 \rangle\rangle = q_0 \int_{t'}^t ds_1 u(s_1) = q_0(t-t')$$

and thus (A1) assumes the form (2.3b).

Along the same arguments the complete integrand

$$\langle H(t', t) \rangle = \langle \mathcal{G}(t-t') F(t') \rangle$$

of (2.2a) is obtained from

$$\langle H(t', t) \rangle = \theta(t-t') \partial_{\epsilon} \langle \exp[\epsilon F(t') - \Lambda(t', t)] \rangle_{\epsilon=0} \quad (A4)$$

as

$$\langle H(t', t) \rangle = \mathcal{G}_1(t-t') F_1(t')$$

where $F_1(t)$ is given by (2.3c).

APPENDIX B

Triple-Correlation Expansion

To expand the triple-correlation (3.4a), consider the averaged product of the Green functions

$$\mathcal{G}_3(t'_1, \dots, t_3) = \langle \mathcal{G}(t_1 - t'_1) \mathcal{G}(t_2 - t'_2) \mathcal{G}(t_3 - t'_3) \rangle$$

first. Analogous to appendix A one obtains

$$\mathcal{G}_3(t'_1, \dots, t_3) = \mathcal{G}_1(t_1 - t'_1) \mathcal{G}_1(t_2 - t'_2) \mathcal{G}_1(t_3 - t'_3) \times \exp[q_0(\tau_{12} + \tau_{13} + \tau_{23})] \quad (B1)$$

where $\tau_{\mu\nu}$ measures the length of the intersection of the time intervals (t'_μ, t_μ) and (t'_ν, t_ν) . Equation (B1) is not a unique expression, unless the time order of all of its six time-parameters has been defined. If all three intervals coincide

$$\mathcal{G}_3(t'_1 = t'_2 = t'_3; t_1 = t_2 = t_3) = \mathcal{G}_{30}(t_1 - t'_1)$$

while

$$\mathcal{G}_3(t'_1, \dots, t_3) = \mathcal{G}_1(t_1 - t'_1) \mathcal{G}_1(t_2 - t'_2) \mathcal{G}_1(t_3 - t'_3)$$

for completely disjoint intervals. To expand the complete integrand of (3.4a) it is rewritten as a single exponential of the form (A4) which then yields to second-order Kubo number

$$\langle h(t'_1, t_1) h(t'_2, t_2) h(t'_3, t_3) \rangle = \mathcal{G}_3(t'_1, \dots, t_3) f_3(t'_1, t'_2, t'_3)$$

with

$$\left. \begin{aligned} f_3(t'_1, t'_2, t'_3) &= \sum_{k=1}^3 f_3^k(t'_1, t'_2, t'_3) \\ f_3^k(t'_1, t'_2, t'_3) &= -q_{01}(t'_k)q_1(t'_i)v_{ij}(t'_k)\delta(t'_i - t'_j) \end{aligned} \right\}$$

where i, j, k denote each a different number out of (1, 2, 3) and

$$v_{ij}(t'_k) = u_i(t'_k) + u_j(t'_k) \quad (\text{B2})$$

is made up by unit indicators of the form of (A3). To perform now the three integrations of (3.4a), it is necessary to specify the chronology completely. Consider the procedure in detail for $k = 3$

$$r_3^3(t_1 \leq t_2 \leq t_3) = \int_{-\infty}^{\infty} d^3 t' \mathcal{G}_3(t'_1, \dots, t'_3) f_3^3(t'_1, t'_2, t'_3).$$

In this case (B2) becomes

$$v_{12}(t'_3) = u_1(t'_3) + u_2(t'_3),$$

and hence

$$\begin{aligned} r_3^3 &= r_3^{30}(t'_1 \leq t_1; t'_2 \leq t'_3 \leq t_2 \leq t_3) \\ &\quad + r_3^{31}(t'_2 \leq t_2; t'_1 \leq t'_3 \leq t_1 \leq t_2 \leq t_3). \end{aligned}$$

The time order in the first term is not yet sufficient to perform the δ integration. Hence it is split into

$$\begin{aligned} r_3^{30} &= r_3^{31}(t'_1 \leq t_1; t'_2 \leq t'_3 \leq t_1 \leq t_2 \leq t_3) \\ &\quad + r_3^{32}(t'_2 \leq t'_3; t'_1 \leq t_1 \leq t'_3 \leq t_2 \leq t_3), \end{aligned}$$

and after the δ integration one has

$$\begin{aligned} r_3^3 &= 2r_3^{31}(t'_2 \leq t'_1 \leq t'_3 \leq t_1 \leq t_2 \leq t_3) \\ &\quad + r_3^{32}(t'_2 \leq t'_1 \leq t_1 \leq t'_3 \leq t_2 \leq t_3). \quad (\text{B3}) \end{aligned}$$

This determines the chronology so that the Green function can be cast into a definite form. For the first term of (B3) one has

$$\tau_{12} = t_1 - t'_1, \quad \tau_{13} = t_1 - t'_3, \quad \tau_{23} = t_2 - t'_3.$$

Thus

$$\begin{aligned} \mathcal{G}_3(t'_2 \leq t'_1 \leq t'_3 \leq t_1 \leq t_2 \leq t_3) \\ = \mathcal{G}_1(t_3 - t_2)\mathcal{G}_{20}(t_2 - t_1)\mathcal{G}_{30}(t_1 - t'_3)\mathcal{G}_{20}(t'_3 - t'_1) \end{aligned}$$

while for the second term

$$\tau_{12} = t_1 - t'_1, \quad \tau_{13} = 0, \quad \tau_{23} = t_2 - t'_3$$

which yields

$$\begin{aligned} \mathcal{G}_3(t'_2 \leq t'_1 \leq t_1 \leq t'_3 \leq t_2 \leq t_3) \\ = \mathcal{G}_1(t_3 - t_2)\mathcal{G}_{20}(t_2 - t'_2)\mathcal{G}_1(t'_3 - t_1)\mathcal{G}_{20}(t_1 - t'_1). \end{aligned}$$

After the final two integrations one arrives at

$$\begin{aligned} r_3^3(t_1 \leq t_2 \leq t_3) &= \mathcal{G}_1(t_3 - t_2) \left[\frac{1}{3} \mathcal{G}_{20}(t_2 - t_1)r_{30}(t_1) - t_{20}(t_1) \right. \\ &\quad \left. \times \int_{t_1}^{t_2} dt'_3 \mathcal{G}_{20}(t_2 - t'_3)\mathcal{G}_1(t'_3 - t_1)q_{01}(t'_3) \right]. \end{aligned}$$

Similarly, one derives for $k = 2$:

$$r_3^2(t_1 \leq t_2 \leq t_3) = r_3^3(t_1 \leq t_2 \leq t_3),$$

and for $k = 1$:

$$r_3^1(t_1 \leq t_2 \leq t_3) = \frac{1}{3} \mathcal{G}_1(t_3 - t_2)\mathcal{G}_{20}(t_2 - t_1)r_{30}(t_1).$$

The sum of these three expressions yields the triple correlation (3.4).

REFERENCES

- Arnold, L., 1974: *Stochastic Differential Equations*. Wiley and Sons.
- Blaauboer, D., G. Komen and J. Reiff, 1982: The behavior of the SST as a response to stochastic latent and sensible heat forcing. *Tellus*, **34**, 17–28.
- deElvira, A., and P. Lemke, 1982: A Langevin equation for stochastic climate models with periodic feedback and forcing variance. *Tellus*, **34**, 313–320.
- Frankignoul, C., and K. Hasselmann, 1977: Stochastic climate models, Part II. *Tellus*, **29**, 298–305.
- Hasselmann, K., 1976: Stochastic climate models, Part I. *Tellus*, **28**, 473–485.
- , and T. Barnett, 1981: Techniques of linear prediction for systems with periodic statistics. *J. Atmos. Sci.*, **38**, 2275–2283.
- , W. Munk and G. MacDonald, 1963: Bispectra of ocean waves. *Symp. on Time Series Analysis*. M. Rosenblatt, Ed., Wiley and Sons, 125–139.
- van Kampen, N., 1981: *Stochastic Processes in Physics and Chemistry*. Amsterdam.
- Leith, C., 1975: Climate response and fluctuation dissipation. *J. Atmos. Sci.*, **32**, 2022–2026.
- Parzen, E., and M. Pagano, 1979: An approach to modelling seasonally stationary time-series. *J. Econometrics*, **9**, 137–153.
- Tukey, J., 1961: What can data analysis and statistics offer today. *Proc. Conf. on Ocean Wave Spectra*. Prentice-Hall, 347–351.